

Interactive comment on “Consistency between Fourier transform and small-volume few-wave decomposition for spectral and spatial variability of gravity waves above a typhoon” by C. I. Lehmann et al.

C. I. Lehmann et al.

c.lehmann@fz-juelich.de

Received and published: 16 May 2012

We thank both reviewers for their helpful and constructive comments.

The minor points will be corrected in the final version following the reviewers suggestions. We here reply first to the two larger points raised by reviewer 2 and then answer the other minor points.

The method is inspired by the study of a potential new infrared limb imager and is therefore applied to a stratospheric GW distribution above a complex GW source. It is

C962

suggested that it can be applied also to e.g. model data for which space-time Fourier analysis is not possible, for instance high-resolution ECMWF data which are provided only at 6 hour sampling. In such cases of complex sources it will reveal both spectral and spatial properties. However, introducing a new analysis method, we should also outline its limitations. The reviewer suggests a possible test case in terms of a single source which generates a wide spectrum of GWs, such as e.g. a single latent heat release pulse. These GWs, having different wave vectors, phase speeds and group velocities, would reach the stratosphere at different locations and times. Unfortunately, we have no such test-case available. However, we can perform another stringent test and construct an artificial spatial distribution obeying universal scaling laws. We first prescribe amplitudes $A(k, l, m)$ according to

$$A(k, l, m) = A_0 \left(\frac{k}{k^*} \right)^p \left(\frac{l}{l^*} \right)^p \left(\frac{m}{m^*} \right)^r$$

with (k, l, m) the respective wavenumbers in (x, y, z) direction, (k^*, l^*, m^*) the “characteristic” (or peak) wavenumbers and p and r the exponents of the power laws. The grid of wavenumbers (k, l, m) follows directly from the size and sampling of the whole data volume. The exponents are chosen $p = 1$ for $k, l < k^*, l^*$ and $p = -5/3$ otherwise and $r = 2$ for small m and $r = -3$ for large m . The spatial distribution is then constructed via FFT by superposing all these waves with random phases. By definition, in this test case the whole spatial domain is completely filled by homogeneous waves. Since the distribution is constructed separable, also 1D FFT in the respective spatial dimension can be applied and the average of all 1D profiles be compared to the S3D method.

Examples shown are for a total volume of 121 x 121 x 105 points with 25 km horizontal and 0.5 km vertical sampling analyzed by S3D cubes of 11 points in the horizontal and 21 points in the vertical. This means that we try to describe a spectrum consisting of 187,200 Fourier components by 2 spectral S3D components varying over 605 loca-

C963

tions. In this case of a spectrum of homogeneous waves we therefore expect serious degradation by the S3D method. In Figure 1 we compare S3D results with 1D Fourier transform averaged over the two remaining spatial directions. Normalization is by Parseval's theorem. Figure 2 compares results of S3D and 3D FFT binned according to horizontal and vertical wavelength.

Figure 1: Comparison of (red) S3D and (black) 1D Fourier transform spectra for (left column) horizontal and (right column) vertical coordinates. The solid lines give the average spectrum, dashed lines for the FT show the standard deviation of all 1D FT spectra in one data set. We have repeated the whole experiment for 100 independent random phase configurations: the according standard deviation is denoted for the S3D method by dashed lines.

Figure 2: Comparison of (left) Fourier transform and (right) S3D spectral intensity versus horizontal ($k^2 + l^2$) and vertical wavenumber.

We achieve the following results: By S3D we find broad spectral distributions peaking at about the position of (k^*, l^*, m^*) . The further the spectral distance of the wave vector from the "characteristic" wave vector the larger is an underestimate by S3D. In particular, for spectral components where the intensity is less than one order of magnitude than the peak value, S3D heavily underestimates the intensities. In addition, S3D also overestimates some vertical wavelengths which are an integer fraction or multiple of the vertical extent of the fitting cube. This behavior is not observed for idealized tests with a limited number of superposed waves nor visible in the typhoon test case. In general, the spectral shape is reproduced better when the "characteristic" wavelengths are larger than the extent of the fitting cube.

Concluding: We think that the most likely reason for the good agreement in the typhoon case is a multitude of different forcing regions, each with their own favorite propagation directions, wavelengths and phase speeds. A consistent spectrum is then formed by the average over these regions. The separation of spectral components by GWs

C964

taking different pathes when propagating upward, may add to this effect. This is a situation which is typical for stratospheric measurements, e.g. made by a future infrared limb imager. In all cases where a sufficiently large ensemble of not-too homogeneous forcing is analyzed, S3D will perform well; homogeneous spectra are moderately well characterized. If homogeneous spectra are expected, Fourier transform is the better choice, provided that the data allow this method. However, if a region is probed by a multitude of independent small-volume measurements and FT therefore cannot be applied, S3D is still a way to estimate the salient spectral features.

We will add these results in an appendix to the manuscript.

Regarding the question on the momentum flux from model winds, we will add a paragraph on page 1771, line 15:

Infering GW momentum flux from temperatures involves the use of GW polarization relations. In order to provide a self consistent test with a single analysis method we also spectrally analyzed the model winds. In case of S3D, the wave vector is determined from the vertical winds and only the amplitudes of the horizontal components are fitted. Momentum flux for a single wave is then calculated according to

$$(F_{px}, F_{py}) = \frac{1}{2} \rho (\hat{u}\hat{w}, \hat{v}\hat{w}); \quad (2)$$

spectra are generated as for temperatures.

Reviewer 1, page 1766, line 5: We add one sentence: For instance, only 1 horizontal wavelength upwind of a mountain range, GW momentum flux is often almost negligible small.

Reviewer 1, page 1770, line 7: It should be j and in equation (5) the sum and y should have index i. This will be corrected.

Reviewer 1: language suggestions: The wording will be changed as suggested.

C965

Reviewer 2: We will add a paragraph at page 1773, line 14:

Additionally momentum flux values calculated directly from the model winds are plotted, labeled “direct wind 360km”: First, the background is removed by subtracting an average over 360 x 360 km in the model domain from each individual value. Then for each altitude the average $\rho \bar{u}'w'$ of the whole domain is calculated. In addition, the dashed lines give the average values of only the positive and only the negative values, respectively. The “direct-wind” results hence do not involve any spectral method.

Reviewer 2, Figures 3 to 6: We will add a sentence to the Figure captions of Figures 3 and 5.

The radial coordinate is phase speed, origin is 0 ms^{-1} , circles give phase speeds of 20 ms^{-1} , 40 ms^{-1} and 60 ms^{-1} .

Reviewer 2: The “pig tail” will be highlighted.

Interactive comment on Atmos. Meas. Tech. Discuss., 5, 1763, 2012.

C966

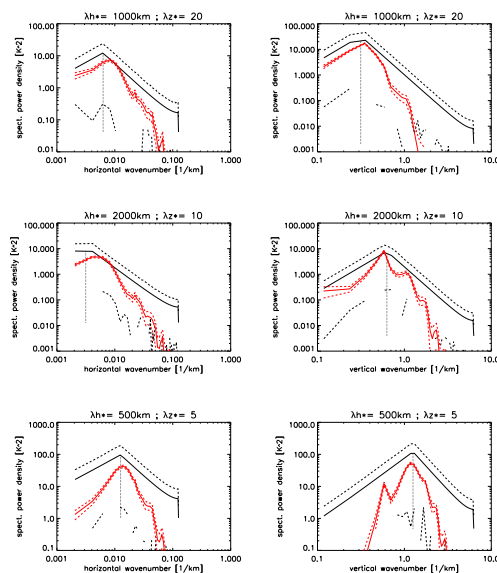


Fig. 1. Comparison of (red) S3D and (black) 1D Fourier transform spectra for (left column) horizontal and (right column) vertical coordinates. The solid lines give the average spectrum, dashed lines for the FT

C967

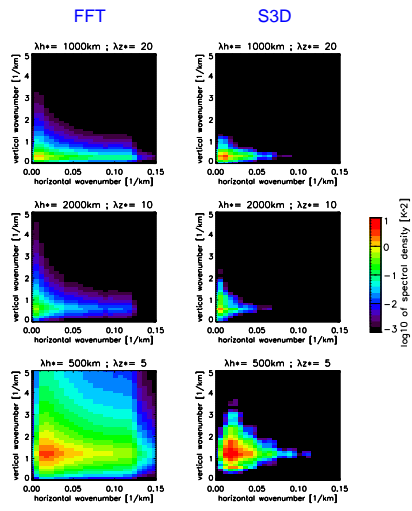


Fig. 2. Comparison of (left) Fourier transform and (right) S3D spectral intensity versus horizontal (k^2+l^2) and vertical wavenumber.